Characterization of coronary atherosclerosis on computed tomography using advanced image processing techniques

PhD Thesis

Márton József Kolossváry MD

Doctoral School of Basic and Translational Medicine
Semmelweis University

Supervisor: Pál Maurovich-Horvat MD, PhD
Official reviewers: Pál Kaposi Novak MD, PhD
Gál Viktor MD, PhD
Head of the Complex Examination Committee:
Tivadar Tulassay MD, PhD
Members of the Complex Examination Committee:
Attila Patócs MD, PhD
Péter Andrkéa MD, PhD

Budapest
2020

1. INTRODUCTION

Despite advancements in the diagnosis and therapy of cardiovascular diseases (CVD), it still remains the leading cause of morbidity and mortality worldwide. Coronary artery disease (CAD), the leading pathology behind CVD is a progressive disease of the intimal layer of the coronaries, which can cause acute and/or chronic luminal obstruction. Coronary CT angiography (CTA) has emerged as a useful and highly reliable imaging modality for the examination of the coronaries and is considered as a non-invasive alternative to invasive coronary angiography (ICA). Even though, numerous studies have validated the diagnostic performance of CTA for the detection of obstructive coronary artery disease, as compared to ICA as reference standard, only a few studies have compared these two modalities regarding semi-quantitative plaque burden measurements.

Modern CT scanners allow not only the visualization of the coronary lumen as ICA, but also the vessel wall granting non-invasive analysis of atherosclerosis itself. The napkin-ring sign (NRS) is a qualitative marker high-risk plaque feature. Due to its qualitative nature, identification of the NRS is affected by clinical experience and inter-reader variability. Therefore, more objective methods of compositional assessment are warranted.

Radiomics is the process of obtaining quantitative parameters from these spatial datasets, in order to create ‘big data’ datasets, where each lesion is characterized by hundreds of different parameters. Application of radiomics in cardiovascular imaging is lacking.

Implementing radiomics with machine learning (ML) and artificial intelligence (AI) may allow to increase the abilities of coronary CTA imaging to allow better identification of vulnerable plaques by localizing plaques with metabolic activity, or by identifying the exact histological category of a given lesion using simple CT images.

The current thesis aims to assess the potentials of advanced image analysis of atherosclerosis using coronary CTA images.

2. OBJECTIVES

2.1. Defining the effect of using coronary CTA to assess coronary plaque burden as opposed to ICA

Our objective was to compare coronary CTA and ICA regarding semi-quantitative plaque burden assessment and to assess the effect of imaging modality on cardiovascular risk classification.

2.2. Defining the potential of using radiomics to identify napkin-ring sign plaques on coronary CTA

As there was no implementation of radiomics to cardiovascular imaging, we sought to assess whether calculation of radiomic features is feasible on coronary lesions. Furthermore, we aimed to evaluate whether radiomic parameters can differentiate between plaques with or without NRS.

2.3. Defining the potential of radiomics to identify invasive and radionuclide imaging markers of vulnerable plaques on coronary CTA

We wished to assess whether coronary CTA radiomics could outperform current standards to identify invasive and radionuclide imaging markers of high-risk plaques described by intravascular ultrasound (IVUS), optical coherence tomography (OCT) and NaF18-Positron Emission Tomography (NaF18-PET).

2.4. Defining the potential effect of image reconstruction algorithms on reproducibility of volumetric and radiomic signatures of coronary lesions on coronary CTA

Our primary aim was to assess whether filtered back projection (FBP), hybrid (HIR) or model-based (MIR) iterative reconstruction have any significant effect on volumetric and radiomic parameters of coronary plaques. Furthermore, we sought to evaluate the impact of the type of binning and the number of bins used for discretization on radiomic parameter values.

2.5. Defining the potential of using radiomic markers as inputs to machine learning models to identify advanced atherosclerotic lesions as assessed by histology

Our objective was to compare the diagnostic performance of radiomics-based ML with visual and histogram-based plaque assessment to identify advanced coronary lesions using histology as reference standard.

3. METHODS

3.1. The effect of using coronary CTA to assess coronary plaque burden as opposed to ICA

Out of the 868 patients enrolled by our institution in the Genetic Loci and the Burden of Atherosclerotic Lesions study (NCT01738828), we selected individuals who underwent both coronary CTA and ICA within 120 days. In total, 71 patients (mean age 61.6±9.0 years, 36.6% female) were included in our analysis. In each patient, segment involvement score (SIS) was used to quantify the number of segments with any plaque, whereas segment stenosis score (SSS) was calculated by summing the stenosis scores of each segment. Based on Bittencourt et al. the extent of CAD was classified as non-extensive (SIS $\leq$ 4) or extensive (SIS > 4) and obstructive (at least one segment with $\geq$50% stenosis) or non-obstructive (no segment with $\geq$50% stenosis).

Patients were classified as extensive obstructive, nonextensive obstructive, extensive nonbostructive or nonextensive nonobstructive based on ICA and also CTA results.

3.2. The potential of using radiomics to identify napkin-ring sign plaques on coronary CTA

From 2674 consecutive coronary CTA examinations due to stable chest pain we retrospectively identified 30 patients who had NRS plaques. As a control group, we retrospectively matched 30 plaques of 30 patients from our clinical database with excellent image quality. We matched the non-NRS group based on degree of calcification and stenosis, plaque localization, tube voltage and image reconstruction. Image segmentation and data extraction was performed using a dedicated software tool for automated plaque assessment (QAngioCT Research Edition; Medis medical imaging systems bv, Leiden, The Netherlands). The voxels containing the plaque tissue were exported as a DICOM dataset using a dedicated software tool (QAngioCT 3D workbench, Medis medical imaging systems bv, Leiden, The Netherlands). We developed an open source software package in the R programing environment (Radiomics Image Analysis (RIA)) which is capable of calculating hundreds of different radiomic parameters on 2D and 3D datasets. We calculated 4440 radiomic features for each coronary plaque using the RIA software tool. Due to the large number of comparisons, we used the Bonferroni correction to account for the family wise error rate.

3.3. The potential of radiomics to identify invasive and radionuclide imaging markers of vulnerable plaques on coronary CTA

The current study is a post-hoc retrospective analysis of patients who have also undergone coronary CTA due to suspected coronary artery disease

between March and October of 2015 within 90 days prior to invasive angiography. In total, 27 patients with at least one moderate (40-70%) stenosis on the proximal or mid-portion of any major coronary artery were included in our study. All patients underwent NaF^{18}-PET and invasive coronary angiography. During the invasive procedure, both IVUS and OCT was performed. Overall, 44 plaques of 25 patients using all four imaging modalities were investigated. Each coronary plaque was segmented using a semi-automated software tool (QAngioCT Research Edition; Medis medical imaging systems bv, Leiden, The Netherlands). Using the segmented datasets, voxels containing plaque were exported as a DICOM image (QAngioCT 3D workbench, Medis medical imaging systems bv, Leiden, The Netherlands). Overall 935 different radiomic parameters were calculated using the RIA software package in the R environment. We conducted a stratified 5-fold cross-validation with 1,000 repeats for our diagnostic accuracy calculations, which decreases the bias of overfitting.

3.4. The effect of image reconstruction algorithms on reproducibility of volumetric and radiomic signatures of coronary lesions on coronary CTA

We retrospectively identified 20 non-calcified, 20 partially calcified and 20 calcified coronary atherosclerotic plaques of 60 patients (age 60.4±9.8; female: 26.6%) showing at least 25% stenosis on excellent image quality coronary CTA scans. An expert reader manually segmented the coronary plaques on HIR image using a dedicated software tool (QAngioCT Research Edition; Medis medical imaging systems bv). Voxels containing plaque tissue were extracted as a DICOM image with dimensions identical to the original image using a dedicated software (QAngioCT 3D workbench, Medis medical imaging systems bv). Radiomic parameters were calculated on all three reconstructions. Radiomic parameters were calculated using with 2, 4, 8, 16, 32, 64, 128 and 256 number of bins both for equally sized and equally probable binning. Beta (β) and p values are reported for each

independent variable. ΔR^2 was calculated for each independent variable by subtracting the R^2 value calculated when considering all variables except the given variable from the regression model which considered all variables. ΔR^2 was calculated as an effect size measure, to show the proportion of variance attributable to a given parameter.

3.5. Using radiomic markers as inputs to machine learning models to identify advanced atherosclerotic lesions as assessed by histology

The fresh donor hearts were imaged without formalin fixation using a 64-detector row CT scanner. Histologic preparation and analysis were performed at a pathology institute that specializes in cardiovascular histopathology. Each cross-section was classified according the modified American Heart Association scheme into the following categories: adaptive intima thickening, pathological intimal thickening, fibrous plaque, early fibroatheroma, late fibroatheroma and the thin cap fibroatheroma. An experienced reader performed the qualitative reading of all coronary CTA cross-sections and classified them based on the traditional and the plaque attenuation pattern scheme. All coronary CTA cross-sections were manually segmented using a dedicated open-source software (3D Slicer v4.8.1., Boston, Massachusetts, open-source). Images were exported in NRRD files and imported into RIA (v1.4.1, Budapest, Hungary, open-source) software package in the R environment. For histogram-based assessment, the area of low attenuation (<30 HU) and the average HU values were calculated from the segmented coronary CTA images. Altogether 1919 radiomic parameters were calculated for each cross-section. All model building was done in the python environment (v3.6.2, Beaverton, Oregon, open-source) using the Scikit-learn package (v0.19.1, open-source). Code used for analysis can be accessed at: https://github.com/martonkolossvary/radiomics_ex-vivo_src

4. RESULTS

4.1. Comparison of quantity of coronary atherosclerotic plaques detected by coronary CTA versus ICA

Coronary CTA detected coronary artery plaque in 49% (487/1000) of the segments, whereas ICA showed coronary plaques in 24% (235/1000) of all segments ($p<0.001$). Of the 235 positive segments with ICA, corresponding segments on CTA was also positive in 94%. When considering the severity of coronary stenosis only seen by CTA, 79% of plaques caused minimal or mild luminal stenosis (211/266). Conversely, ICA detected plaque only in 3% (14/513) of segments where CTA was negative. Regarding segment scores, CTA showed more than two times as many segments with plaque compared to ICA, and also the overall degree of stenosis caused by the plaques was almost twice.

Out of 71 patients, based on CTA results 72% (51/71) was classified as extensive obstructive, 3% (2/71) as extensive non-obstructive, 13% (9/71) as non-extensive obstructive and 13% (9/71) as non-extensive non-obstructive. Using ICA based measurements, 27% (19/71) of the patients was extensive obstructive, 1% (1/71) was extensive non-obstructive, 49% (35/71) was non-extensive obstructive and 23% (16/71) was non-extensive non-obstructive. Overall 52% (37/71) of the patients moved to a higher risk category, while 1% (1/71) moved to a lower category using CTA based measurements as compared to ICA based measurements.

4.2. Identification of napkin-ring sign plaques using radiomics

Overall, 4440 radiomic parameters were calculated for each atherosclerotic lesion. Out of all calculated radiomic parameters, 20.6% (916/4440) showed a significant difference between plaques with or without NRS (all

p<0.0012). Of the 44 calculated first-order statistics 25.0% (11/44) was significant. Out of the 3585 calculated GLCM statistics 20.7% (742/3585) showed a significant difference between the two groups. Among the 55 GLRLM parameters 54.5% (30/55) were significant, while 17.6% (133/756) of the calculated 756 geometry-based parameters had a p<0.0012. A Manhattan plot of the p values of the calculated radiomic parameters is shown in figure 1.

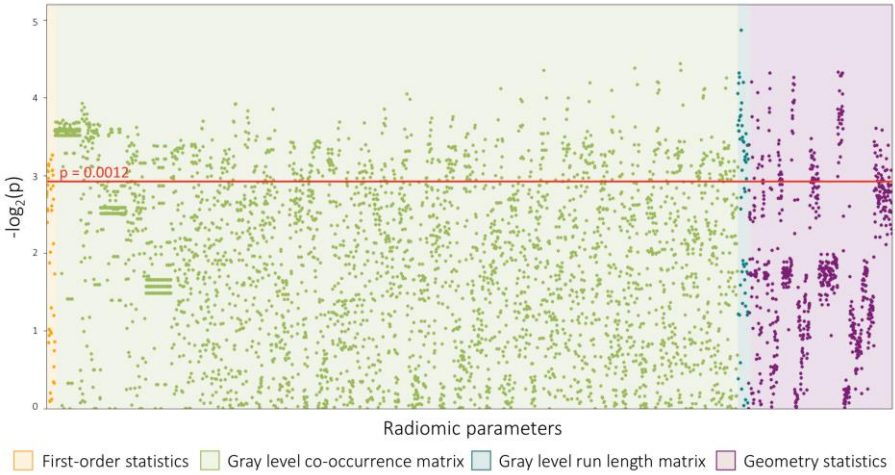

Figure 1. *Manhattan plot of all 4440 calculated p values.*
The Manhattan plot shows all 4440 calculated p values comparing napkin-ring sign (NRS) vs. non-NRS plaques and their distribution among the different classes of radiomic parameters.

4.3. Identification of invasive and radionuclide imaging markers of vulnerable plaques using radiomic analysis of coronary CTA

Overall, 44 plaques were analysed; 30/44 (68.2%) plaques showed attenuation on IVUS, 7/44 (15.9%) showed TCFA on OCT and in 11/44

(25.0%) cases >25% NaF^{18} uptake was present. All plaques which were TCFA by OCT also showed attenuation on IVUS. Out of the 30 attenuated plaques 8/30 (26.7%) showed radionuclide uptake on NaF^{18}-PET, however none of the TCFA plaques showed >25% NaF^{18} uptake. Among radiomic metrics, 35/935 (3.7%) had AUC values between 0.70 and 0.79 and 311/935 (33.3%) had values between 0.60-0.69 to identify IVUS-attenuated plaque. Overall, 1/935 (0.1%) of all radiomic parameters had AUC values between 0.80-0.89, 44/935 (4.7%) between 0.70-0.79 and 219/935 (23.4%) had values between 0.60 and 0.69 to identify OCT-TCFA. Overall, 30/935 (3.2%) of the radiomic parameters had AUC values between 0.80 and 0.89, 331/935 (35.4%) had values between 0.70-0.79 and 232/935 (24.8%) had values between 0.60-0.69 to identify NaF^{18}-positivitiy (figure 2).

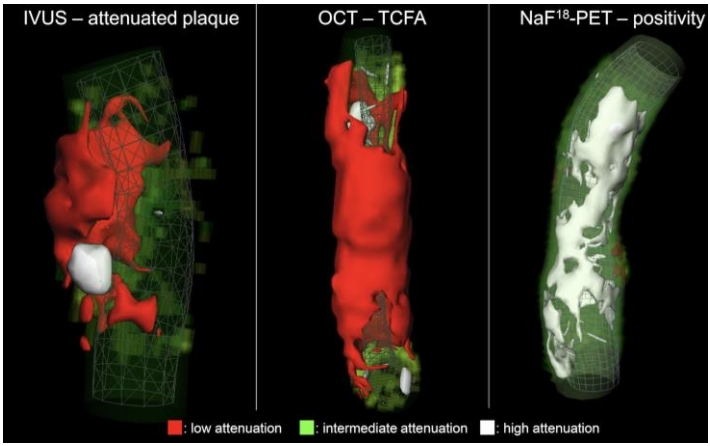

Figure 2. *Representative volume rendered CT images of three coronary plaques corresponding to specific invasive and radionuclide imaging markers of plaque vulnerability.*
IVUS: intravascular ultrasound; NaF^{18}-PET: Sodium-floride positron emission tomography; OCT: optical coherence tomography

4.4. Effect of image reconstruction algorithms on volumetric and radiomics features derived from coronary CTA

Aorta SD, CNR and SNR had low ICC values between image reconstructions (0.46, 0.60, 0.63; respectively), while lumen and pericoronary fat mean HU had excellent and good reproducibility (0.99, 0.83; respectively). Image reconstruction had a significant effect on aorta SD, CNR and SNR values with large ΔR^2, while lumen or pericoronary fat mean HU values were unaffected by the different algorithms. Linear regression analysis showed that the type of binning i.e equal sized or equally probable binning, was a significant predictor of radiomic values for 90% (103/114) of all GLCM parameters. Among GLCM parameters ΔR^2 values attributable to the type of binning were smaller than 0.25 in 87% (99/114) of the radiomic parameters. 3% (3/114) had ΔR^2 changes between 0.25 and 0.49, and 2% (2/114) had changes between 0.50 and 0.75. Even though all GLRLM parameters were significantly affected by binning type ($p<0.05$, all), the ΔR^2 attributable to adding binning type to the regression model only minimally changed the R^2 values ($\Delta R^2 <0.04$ for all). The number of bins to which HU values were discretized before the calculation of radiomic parameters, significantly affected the values for all GLCM and GLRLM parameters. Among GLCM, 61% (70/114) of the parameters had a $\Delta R^2 <0.25$ if the number of bins was added to the model. 16% (18/114) produced ΔR^2 between 0.25 and 0.49, 17% (19/114) between 0.50-0.74 and 6% (7/114) of all parameters had R^2 change values greater than 0.75. Regarding GLRLM parameters, 4 parameters' ΔR^2 was less than 0.25 when the number of bins was added to the regression model. 4 statistics produced R^2 changes between 0.25 and 0.49, while in case of 3 parameters the ΔR^2 was more than 0.75.

4.5. Identification of advanced atherosclerotic images using radiomics-based machine learning validated using histology

Overall, 611 histological sections from 21 coronary arteries of 7 donor hearts were investigated. The dataset was randomly split into a training-set (75%, 333/445) and a validation-set (25%, 112/445). Among radiomics-based ML models, the least angles regression model provided the best discriminatory power on the training-set. The radiomics-based ML model achieved good diagnostic accuracy (AUC=0.73, CI: 0.63-0.84) on the validation-set. The plaque attenuation pattern scheme achieved moderate diagnostic accuracy, AUC=0.65, CI: 0.56-0.73, while histogram-based measurements: area of low attenuation (<30 HU) and the average HU values of the plaque cross-sections produced poor diagnostic accuracy (AUC=0.55, CI: 0.42-0.68, AUC=0.53, CI: 0.42-0.65; respectively) on the validation-set. The radiomics-based ML model outperformed expert visual assessment (AUC=0.73 vs. 0.65; p=0.04) and also histogram-based measurements, such as area of low attenuation (<30 HU) (AUC=0.73 vs. 0.55, p=0.01) and the average HU values of the plaque cross-sections (AUC=0.73 vs. 0.53, p=0.004). Results are summarized in figure 3.

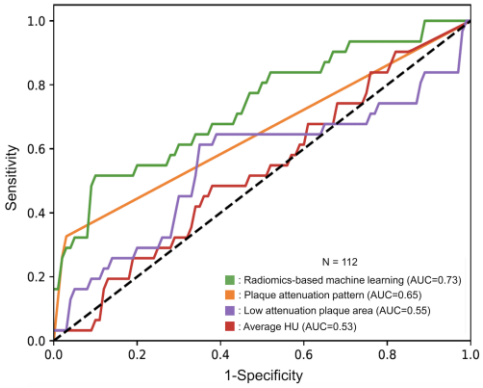

Figure 3. *Receiver operating characteristics curves of radiomics-based machine learning model, plaque attenuation pattern, area of low attenuation and average HU value to identify advanced atherosclerotic lesions.*

5. CONCLUSIONS

Coronary CTA has emerged as the first line of choice for the evaluation of CAD in stable patients. Based-on our results it seems, coronary CTA is superior to ICA to describe the overall amount of CAD in these patients, and therefore may provide a more accurate method for risk stratification. Furthermore, coronary CTA provides imaging of not only the luminal stenosis, but the atherosclerotic disease itself. This provides a unique opportunity to apply advanced image analysis such as radiomics to precision phenotype CAD.

Radiomic analysis of coronary plaques showed that we can identify NRS plaques with good diagnostic accuracy, showing that imaging markers currently only identifiable visually by radiologists may be identified objectively using mathematical formulas. We have also showed that radiomic analysis has the potential not only to identify imaging markers of CT, but also to identify metabolic activity currently only detectable using PET imaging. Furthermore, our results indicate that radiomics may have the potential to overcome the spatial resolution limitations of CT, as it may be able to identify invasive imaging markers currently only identifiable using IVUS and OCT. Also, using radiomic parameters as inputs to machine learning models we were able to classify coronary CTA cross-sections as being advanced lesions based-on histology. This may allow the exact pathological classification of diseases rather than indirect classifications with differing accuracies currently used in radiology. As with all emerging technologies, reproducibility and robustness are always a question. Our results indicate, that different image reconstruction techniques have little effect on radiomic parameters values indicating that radiomics may be robust to different scanner settings.

New image analytic techniques such as radiomics, will reshape the field of cardiac imaging. This has the potential to increase our understanding of CAD and provide more precise diagnostics and prognostication. However, these techniques are still in their infancy. Nevertheless, as fast as AI is transforming our everyday lives, these changes may come sooner than later.

6. CANDIDATE'S PUBLICATIONS

6.1. Publications discussed in the present thesis

1. **Kolossvary M**, Szilveszter B, Edes IF, Nardai S, Voros V, Hartyanszky I, Merkely B, Voros S, Maurovich-Horvat P. (2016) Comparison of Quantity of Coronary Atherosclerotic Plaques Detected by Computed Tomography Versus Angiography. Am J Cardiol, 117: 1863-1867. ***IF: 3.398***
2. **Kolossvary M**, Karady J, Szilveszter B, Kitslaar P, Hoffmann U, Merkely B, Maurovich-Horvat P. (2017) Radiomic Features Are Superior to Conventional Quantitative Computed Tomographic Metrics to Identify Coronary Plaques With Napkin-Ring Sign. Circ Cardiovasc Imaging, 10. ***IF: 6.221***
3. **Kolossvary M**, Park J, Bang JI, Zhang J, Lee JM, Paeng JC, Merkely B, Narula J, Kubo T, Akasaka T, Koo BK, Maurovich-Horvat P. (2019) Identification of invasive and radionuclide imaging markers of coronary plaque vulnerability using radiomic analysis of coronary computed tomography angiography. Eur Heart J Cardiovasc Imaging, 20: 1250-1258. ***IF: 5.260***
4. **Kolossvary M**, Szilveszter B, Karady J, Drobni ZD, Merkely B, Maurovich-Horvat P. (2019) Effect of image reconstruction algorithms on volumetric and radiomic parameters of coronary plaques. J Cardiovasc Comput Tomogr, 13: 325-330. ***IF: 3.316***
5. **Kolossvary M**, Karady J, Kikuchi Y, Ivanov A, Schlett CL, Lu MT, Foldyna B, Merkely B, Aerts HJ, Hoffmann U, Maurovich-Horvat P. (2019) Radiomics versus Visual and Histogram-based Assessment to Identify Atheromatous Lesions at Coronary CT Angiography: An ex Vivo Study. Radiology, 293: 89-96. ***IF: 7.608***

6.2. Publications not related to the present thesis

1. Bagyura Z, **Kolossvary M**, Merkely B, Maurovich-Horvat P. (2017) [Computer tomography examination of the coronary system - National Plaque Registry and Database, Hungary]. Orv Hetil, 158: 106-110. ***IF: 0.322***
2. Bagyura Z, **Kolossváry M**, Merkely BP, Maurovich-Horvat P. (2015) Személyre szabott kardiovaszkuláris rizikóbecslés koronária CT-vel Strukturált leletezés és az OPeRA (Országos Plaque Regiszter és Adatbázis) Projekt. IME: INTERDISZCIPLINÁRIS MAGYAR EGÉSZSÉGÜGY / INFORMATIKA ÉS MENEDZSMENT AZ EGÉSZSÉGÜGYBEN, 14: 19-23. ***IF: 0.000***
3. Banga PV, Varga A, Csobay-Novak C, **Kolossvary M**, Szanto E, Oderich GS, Entz L, Sotonyi P. (2018) Incomplete circle of Willis is associated with a higher incidence of neurologic events during carotid eversion endarterectomy without shunting. J Vasc Surg, 68: 1764-1771. ***IF: 3.243***
4. Barta H, Jermendy A, **Kolossvary M**, Kozak LR, Lakatos A, Meder U, Szabo M, Rudas G. (2018) Prognostic value of early, conventional proton magnetic resonance spectroscopy in cooled asphyxiated infants. BMC Pediatr, 18: 302. ***IF: 1.983***
5. Bartykowszki A, **Kolossvary M**, Jermendy AL, Karady J, Szilveszter B, Karolyi M, Balogh O, Sax B, Merkely B, Maurovich-Horvat P. (2018) Image Quality of Prospectively ECG-Triggered Coronary CT Angiography in Heart Transplant Recipients. AJR Am J Roentgenol, 210: 314-319. ***IF: 3.161***
6. Bencsik P, Sasi V, Kiss K, Kupai K, **Kolossvary M**, Maurovich-Horvat P, Csont T, Ungi I, Merkely B, Ferdinandy P. (2015) Serum lipids and cardiac function correlate with nitrotyrosine and MMP activity in coronary artery disease patients. Eur J Clin Invest, 45: 692-701. ***IF: 2.687***
7. Bikov A, **Kolossvary M,** Jermendy AL, Drobni ZD, Tarnoki AD, Tarnoki DL, Forgo B, Kovacs DT, Losonczy G, Kunos L, Voros S, Merkely B, Maurovich-Horvat P. (2019) Comprehensive coronary plaque assessment in patients with obstructive sleep apnea. J Sleep Res, 28: e12828. ***IF: 3.432***

8. Celeng C, **Kolossvary M**, Kovacs A, Molnar AA, Szilveszter B, Horvath T, Karolyi M, Jermendy AL, Tarnoki AD, Tarnoki DL, Karady J, Voros S, Jermendy G, Merkely B, Maurovich-Horvat P. (2017) Aortic root dimensions are predominantly determined by genetic factors: a classical twin study. Eur Radiol, 27: 2419-2425. ***IF: 4.027***
9. Csobay-Novak C, Fontanini DM, Szilagyi B, Szeberin Z, **Kolossvary M**, Maurovich-Horvat P, Huttl K, Sotonyi P. (2017) Thoracic Aortic Strain is Irrelevant Regarding Endograft Sizing in Most Young Patients. Ann Vasc Surg, 38: 227-232. ***IF: 1.363***
10. Donnelly PM, **Kolossvary M**, Karady J, Ball PA, Kelly S, Fitzsimons D, Spence MS, Celeng C, Horvath T, Szilveszter B, van Es HW, Swaans MJ, Merkely B, Maurovich-Horvat P. (2018) Experience With an On-Site Coronary Computed Tomography-Derived Fractional Flow Reserve Algorithm for the Assessment of Intermediate Coronary Stenoses. Am J Cardiol, 121: 9-13. ***IF: 2.843***
11. Drobni ZD, **Kolossvary M**, Karády J, Jermendy Á, Littvay L, Tárnoki ÁD, Tárnoki DL, Voros S, Jermendy G, Merkely B, Maurovich-Horvat P. (2017) Van-e összefüggés az epikardiális zsírszövet és a koszorúér-betegség között? Cardiologia Hungarica, 47: 25-29. ***IF: 0.000***
12. Drobni ZD, **Kolossvary M**, Szilveszter B, Merkely B, Maurovich-Horvat P. (2018) A koronária-CT-angiográfia jelentősége a mindennapi gyakorlatban stabil anginás betegek körében. Cardiologia Hungarica, 48: 52-57. ***IF: 0.000***
13. Fontanini DM, Fazekas G, Vallus G, Juhasz G, Varadi R, Kovesi Z, **Kolossvary M**, Szeberin Z. (2018) [Thoracic aortic stentgraft implantations in Hungary from 2012 to 2016]. Orv Hetil, 159: 53-57. ***IF: 0.564***
14. Jermendy AL, **Kolossvary M**, Drobni ZD, Tarnoki AD, Tarnoki DL, Karady J, Voros S, Lamb HJ, Merkely B, Jermendy G, Maurovich-Horvat P. (2018) Assessing genetic and environmental influences on epicardial and abdominal adipose tissue quantities: a classical twin study. Int J Obes (Lond), 42: 163-168. ***IF: 4.514***

15. Karády J, Drobni ZD, **Kolossvary M**, Maurovich-Horvat P. (2015) Non-invasive Assessment of Coronary Plaque Morphology. Current Radiology Reports, 3. ***IF: 0.000***
16. Karady J, Panajotu A, **Kolossvary M**, Szilveszter B, Jermendy AL, Bartykowszki A, Karolyi M, Celeng C, Merkely B, Maurovich-Horvat P. (2017) The effect of four-phasic versus three-phasic contrast media injection protocols on extravasation rate in coronary CT angiography: a randomized controlled trial. Eur Radiol, 27: 4538-4543. ***IF: 4.027***
17. Karolyi M, **Kolossvary M**, Bartykowszki A, Kocsmar I, Szilveszter B, Karady J, Merkely B, Maurovich-Horvat P. (2019) Quantitative CT assessment identifies more heart transplanted patients with progressive coronary wall thickening than standard clinical read. J Cardiovasc Comput Tomogr, 13: 128-133. ***IF: 3.316***
18. Karolyi M, Szilveszter B, **Kolossvary M**, Takx RA, Celeng C, Bartykowszki A, Jermendy AL, Panajotu A, Karady J, Raaijmakers R, Giepmans W, Merkely B, Maurovich-Horvat P. (2017) Iterative model reconstruction reduces calcified plaque volume in coronary CT angiography. Eur J Radiol, 87: 83-89. ***IF: 2.843***
19. **Kolossvary M**, Szilveszter B, Merkely B, Maurovich-Horvat P. (2017) Plaque imaging with CT-a comprehensive review on coronary CT angiography based risk assessment. Cardiovasc Diagn Ther, 7: 489-506. ***IF: 0.000***
20. **Kolossvary M**, Szekely AD, Gerber G, Merkely B, Maurovich-Horvat P. (2017) CT Images Are Noninferior to Anatomic Specimens in Teaching Cardiac Anatomy-A Randomized Quantitative Study. J Am Coll Radiol, 14: 409-415 e402. ***IF: 3.393***
21. **Kolossvary M**, Kellermayer M, Merkely B, Maurovich-Horvat P. (2018) Cardiac Computed Tomography Radiomics: A Comprehensive Review on Radiomic Techniques. J Thorac Imaging, 33: 26-34. ***IF: 2.078***
22. **Kolossvary M**, De Cecco CN, Feuchtner G, Maurovich-Horvat P. (2019) Advanced atherosclerosis imaging by CT: Radiomics,

machine learning and deep learning. J Cardiovasc Comput Tomogr, 13: 274-280. ***IF: 3.316***

23. Korosi B, Vecsey-Nagy M, **Kolossvary M**, Nemcsik-Bencze Z, Szilveszter B, Laszlo A, Batta D, Gonda X, Merkely B, Rihmer Z, Maurovich-Horvat P, Eorsi D, Torzsa P, Nemcsik J. (2019) Association between Cyclothymic Affective Temperament and Age of Onset of Hypertension. Int J Hypertens, 2019: 9248247. ***IF: 1.865***
24. Kovacs A, Molnar AA, **Kolossvary M**, Szilveszter B, Panajotu A, Lakatos BK, Littvay L, Tarnoki AD, Tarnoki DL, Voros S, Jermendy G, Sengupta PP, Merkely B, Maurovich-Horvat P. (2018) Genetically determined pattern of left ventricular function in normal and hypertensive hearts. J Clin Hypertens (Greenwich), 20: 949-958. ***IF: 2.444***
25. Kovacs K, Szakmar E, Meder U, **Kolossvary M**, Bagyura Z, Lamboy L, Elo Z, Szabo A, Szabo M, Jermendy A. (2017) [Hypothermia treatment in asphyxiated neonates - a single center experience in Hungary]. Orv Hetil, 158: 331-339. ***IF: 0.322***
26. Lakatos A, **Kolossvary M**, Szabo M, Jermendy A, Bagyura Z, Barsi P, Rudas G, Kozak LR. (2018) Novel structured MRI reporting system in neonatal hypoxic-ischemic encephalopathy - issues of development and first use experiences. Ideggyogy Sz, 71: 265-276. ***IF: 0.113***
27. Lakatos A, **Kolossvary M**, Szabo M, Jermendy A, Barta H, Gyebnar G, Rudas G, Kozak LR. (2019) Neurodevelopmental effect of intracranial hemorrhage observed in hypoxic ischemic brain injury in hypothermia-treated asphyxiated neonates - an MRI study. BMC Pediatr, 19: 430. ***IF: 1.983***
28. Maurovich-Horvat P, Tarnoki DL, Tarnoki AD, Horvath T, Jermendy AL, **Kolossvary M**, Szilveszter B, Voros V, Kovacs A, Molnar AA, Littvay L, Lamb HJ, Voros S, Jermendy G, Merkely B. (2015) Rationale, Design, and Methodological Aspects of the BUDAPEST-GLOBAL Study (Burden of Atherosclerotic Plaques

Study in Twins-Genetic Loci and the Burden of Atherosclerotic Lesions). Clin Cardiol, 38: 699-707. ***IF: 2.431***

29. Nemcsik J, Vecsey-Nagy M, Szilveszter B, **Kolossvary M**, Karady J, Laszlo A, Korosi B, Nemcsik-Bencze Z, Gonda X, Merkely B, Rihmer Z, Maurovich-Horvat P. (2017) Inverse association between hyperthymic affective temperament and coronary atherosclerosis: A coronary computed tomography angiography study. J Psychosom Res, 103: 108-112. ***IF: 2.947***
30. Szelid Z, Lux A, **Kolossvary M**, Toth A, Vago H, Lendvai Z, Kiss L, Maurovich-Horvat P, Bagyura Z, Merkely B. (2015) Right Ventricular Adaptation Is Associated with the Glu298Asp Variant of the NOS3 Gene in Elite Athletes. PLoS One, 10: e0141680. ***IF: 3.057***
31. Szilveszter B, Elzomor H, Karolyi M, **Kolossvary M**, Raaijmakers R, Benke K, Celeng C, Bartykowszki A, Bagyura Z, Lux A, Merkely B, Maurovich-Horvat P. (2016) The effect of iterative model reconstruction on coronary artery calcium quantification. Int J Cardiovasc Imaging, 32: 153-160. ***IF: 1.896***
32. Szilveszter B, **Kolossvary M**, Karady J, Jermendy AL, Karolyi M, Panajotu A, Bagyura Z, Vecsey-Nagy M, Cury RC, Leipsic JA, Merkely B, Maurovich-Horvat P. (2017) Structured reporting platform improves CAD-RADS assessment. J Cardiovasc Comput Tomogr, 11: 449-454. ***IF: 3.095***
33. Szilveszter B, Nagy AI, Vattay B, Apor A, **Kolossvary M**, Bartykowszki A, Simon J, Drobni ZD, Toth A, Suhai FI, Merkely B, Maurovich-Horvat P. (2019) Left ventricular and atrial strain imaging with cardiac computed tomography: Validation against echocardiography. J Cardiovasc Comput Tomogr, 2019: 1-7. ***IF: 3.316***
34. Szilveszter B, Oren D, Molnar L, Apor A, Nagy AI, Molnar A, Vattay B, **Kolossvary M**, Karady J, Bartykowszki A, Jermendy AL, Suhai FI, Panajotu A, Maurovich-Horvat P, Merkely B. (2019) Subclinical leaflet thrombosis is associated with impaired reverse remodelling after transcatheter aortic valve implantation. Eur Heart

J Cardiovasc Imaging, In press: In press. doi: 10.1093/ehjci/jez256. ***IF: 5.260***

35. Varga A, Di Leo G, Banga PV, Csobay-Novak C, **Kolossvary M**, Maurovich-Horvat P, Huttl K. (2019) Multidetector CT angiography of the Circle of Willis: association of its variants with carotid artery disease and brain ischemia. Eur Radiol, 29: 46-56. ***IF: 3.962***